A Poloxamer-407 modified liposome encapsulating epigallocatechin-3-gallate in the presence of magnesium: Characterization and protective effect against oxidative damage

A Poloxamer-407 modified liposome encapsulating epigallocatechin-3-gallate in the presence of magnesium: characterization and protective effect against oxidative damage.

Cristina Minnelli[1], Paolo Moretti[1], Gianluca Fulgenzi[2], Paolo Mariani[1], Emiliano Laudadio[1], Tatiana Armeni[3], Roberta Galeazzi[1], Giovanna Mobbili[1]*

[1] Dipartimento di Scienze della Vita e dell'Ambiente (DISVA), Università Politecnica delle Marche, via Brecce Bianche, 60131 Ancona –ITALY
[2] Dipartimento di Scienze Cliniche e Molecolari, Università Politecnica delle Marche, Via Conca, Torrette Polo scientifico didattico Murri, 60131 Ancona –ITALY
[3] Dipartimento Scienze Cliniche Specialistiche ed Odontostomatologiche, Università Politecnica delle Marche, via Brecce Bianche, 60131 Ancona –ITALY
* Correspondence; g.mobbili@staff.univpm.it; +390712204707

Abstract: Epigallocatechin-3-gallate (EGCG) is a polyphenolic catechin from green tea, well known for being bioactive in age-associated pathologies where oxidative stress plays a preeminent role. The activity of this molecule is however contrasted by its high chemical and metabolic instability that determines a poor concentration of the antioxidant within the biological system after administration. In order to protect the molecule and increase its delivery efficiency, we have encapsulated EGCG inside anionic liposomes made of 1-palmitoyl-2-oleoyl-sn-glycero-3-phosphocholine, 1,2-dioleoyl-sn-glycero-3-phosphoethanolamine and cholesteryl hemisuccinate. To maximize EGCG internalization, magnesium salt was added in the preparation. However stable nanodispersions suitable for drug delivery were obtained only after treatment with Poloxamer-407, a polyethylene–propylene glycol copolymer. The structural and morphological properties of the produced dispersion were studied by X-ray diffraction, which showed a multilamellar structure even after EGCG addition and an ordering effect of Poloxamer-407; Dynamic Light Scattering demonstrated serum stability of the liposomes. The characterization was completed by evaluating both encapsulation efficiency (100%, in the final formulation) and *in vitro* EGCG release. Since oxidative stress is involved in numerous retinal degenerative diseases, such as age-related macular degeneration, the ability of these liposomes to contrast H_2O_2-induced cell death was assessed in human retinal cells. Morphological changes at the subcellular level were analyzed by Transmission Electron Microscopy, which showed that mitochondria were better preserved in cells treated with liposomes then those treated with free EGCG. In conclusion, the results demonstrated that the produced formulation enhances the efficacy of EGCG under stress conditions, thus representing a potential formulation for the intracellular delivery of EGCG in diseases caused by oxidative damage.

Keywords: liposomes; oxidative damage; Epigallocatechin-3-gallate; Poloxamer-407; drug delivery; X-ray diffraction.

Introduction

Oxidative stress can be linked to several pathophysiological processes including neurodegenerative (Kim et al., 2015), cardiovascular diseases (Heitzer et al., 2001), cancer (Milkovic et al., 2014), aging (Gil del Valle et al., 2015), obesity (Marseglia et al., 2014), chronic inflammatory disorders like rheumatoid arthritis (Tak et al., 2000) and with several retinal degenerative diseases, such as age-related macular degeneration (AMD) where an increase in the steady-state concentration of reactive oxygen species (ROS) is present (Hernández-Zimbrón et al., 2018). A possible strategy to contrast oxidative stress is to reduce the concentration of ROS, like superoxide anion, hydrogen peroxide, and hydroxyl radical, by enhancing the level of antioxidant molecules in the tissues.

Amongst the water-soluble antioxidants, catechins, the main polyphenolic compounds present in green tea, show considerable bioactivity in degenerative diseases associated with oxidative stress (Mandel et al., 2011; Frei et al., 2003). Epigallocatechin-3-gallate (EGCG), the major constituent in green tea, is mainly responsible for the remarkable antioxidant activity due to the presence of the D ring in the galloyl group in addition to the other three rings present in its structure (A, B and C) (**Figure 1**) which are sensitive to oxidation. (Severino et al., 2009). These structural characteristics account for EGCG's potent radical scavenging activity (Zhang et al., 2007; Nanjo et al., 1999) towards both superoxide and hydroxyl radicals as well as peroxyl radicals, nitric oxide, carbon-centered free radicals and lipid free radicals (Salah et al., 1995;).

.

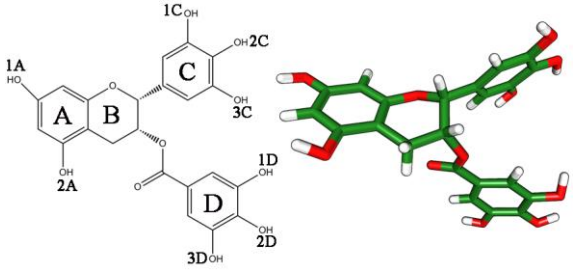

Figure 1. Structure of epigallocatechin-3-gallate (EGCG)

In addition, EGCG can chelate metal ions like copper (II) and iron (III) which participate in the Fenton reaction and are responsible of the subsequent generation of ROS (Morel et al., 1993).

A possible setback in the employment of EGCG as antioxidant is its chemical and metabolic instability, which can determine a low concentration of the antioxidant within the biological system after administration (Lambert and Yang, 2003; Chen et al., 2001). Therefore, the bioavailability of EGCG may be modulated by using nano- or microparticles (Hu et al., 2013; Granja et al., 2017).

Among all drug delivery systems, liposomes offer several advantages because of their biocompatibility, their low toxicity and non-immunogenicity (Torchilin, 2005; Minnelli et al., 2018; Galeazzi et al., 2015; Mobbili et al., 2015; Crucianelli et al., 2014). These supramolecular aggregates can encapsulate enzymatic antioxidants but also hydrophilic and lipophilic chemical antioxidants, shielding and protecting them from inactivation or rapid clearance from cells. Moreover, the ability of polyphenols to interact with the lipid bilayer (Laudadio et al., 2018; Nakayama et al., 2000) promotes the encapsulation of these compounds inside lipidic nanoparticles and makes liposomes potential delivery systems for EGCG (Mignet et al., 2013).

Previously, we used an *in silico* approach combined with experimental methods to identify the best lipid matrix and salt composition for obtaining the highest percentage of encapsulated catechin inside liposomes (Laudadio et al., 2018; Laudadio et al., 2017). In particular, by using anionic multilamellar liposomes prepared from a ternary, lipidic system (POPC/ DOPE /CHEMS 1:1:1) in the presence of Mg^{2+} ions, we obtained complete EGCG encapsulation. However, the liposomes resulted very unstable, as the simultaneous presence of EGCG and magnesium salts was observed to induce the formation of large cluster aggregates.

In order to obtain nanoparticles useful for EGCG delivery applications in this study we describe the preparation and characterization of liposomes made from the same ternary lipidic system, containing EGCG and magnesium salts in addition to a stabilizing agent (the Poloxamer-407) which is able to prevent aggregation and to promote the formation of stable nanodispersions. The structural characteristics of the produced nanodispersions, as well as their *in serum* stability, encapsulation efficiency and *in vitro* EGCG release, were fully determined by different techniques such as X-ray diffraction, dynamic light scattering (DLS), gel filtration and dialysis methods. Moreover, the *in vitro* ability of the nanodispersion to contrast the consequence of H_2O_2 exposure in Adult Retinal Pigmented Epithelium (ARPE-19) cells was evaluated. In particular, the morphological changes in the cytoplasm, mitochondria, endoplasmic reticulum and nucleus of cells induced by the oxidative stress were analyzed by Transmission Electron Microscopy (TEM) while cell viability was assessed by the MTT assay. Since ARPE-19 cells are considered a good *in vitro* model for studying age-related macular degeneration (AMD) (Zareba et al., 2006), the results are very promising in AMD prevention.

It is noteworthy that Poloxamer-407 is a non-ionic triblock copolymer composed by a central hydrophobic poly(propylene oxide) chain (PPO) capped by two hydrophilic chains of poly(ethylene oxide) (PEO), which functions as emulsifier and stabilizer (Wu et al., 2009; Müller et al., 1996;). Poloxamer-407 is approved as an inactive ingredient by the FDA for various types of pharmaceutical formulations, and is accepted as GRAS (Generally Recognized as Safe) excipient (Dumortier et al., 2006), making it an excellent candidate for the preparation of drug delivery systems.

Materials and Methods

Materials

1,2-dioleoyl-*sn*-glycero-3-phosphoethanolamine (DOPE), 1-palmitoyl-2-oleoyl-*sn*-glycero-3-phosphocholine (POPC) and cholesteryl hemisuccinate (CHEMS), used for liposome preparation, were purchased from Avanti Polar Lipids Inc. (Alabaster, AL, USA). Sephadex G-50, Poloxamer-407, $MgCl_2$ salt, 3-(4,5-dimethylthiazol-2-yl-2,5-diphenyl tetrazolium bromide (MTT), hydrogen peroxide and all solvents were obtained from Sigma Aldrich (St. Louis, MO, USA) and used without further purification. Epigallocatechin 3-Gallate was purchased from Cayman Chemical Company (Ann Arbor, MI, USA).

Adult human retinal pigment epithelial (ARPE-19) cells were a kind gifted from Dr. Dario Rusciano (Sooft Italia spa). All cell culture reagents were purchased from Euroclone (Euroclone, Italy). All other chemicals and buffer components were analytical grade preparations.

Preparation of bulk and nanodispersed liposomal phases.

Bulk liposomal phases were obtained by Reverse Phase Evaporation (REV) (Szoka and Papahadjopoulos, 1978). Appropriate amounts of chloroform solutions of DOPE, POPC, CHEMS and methanol solution of EGCG, when present, were mixed to obtain 1:1:1:0.6 mol/mol ratio and a final concentration of 3 mg mL^{-1} of lipids and 1 mM of EGCG. The solvent was removed under reduced pressure at room temperature to preserve the EGCG molecular structure (Price and Spitzer, 1994). After removal of residual solvent under nitrogen flow, lipids were redissolved in 3 mL of an ether/methanol mixture (2:1, v/v) and 1 mL of phosphate buffered saline (PBS, pH 7.4) was added with or without $MgCl_2$ salts ($MgCl_2$/EGCG, 5:1 mol/mol). With the aim to obtain an initial water-in-oil emulsion (W/O), the resulting two-phase system was briefly sonicated (2 min) with a vibra cell sonicator (Sonics Vibra Cell Mod. VCx130) equipped with a tapered micro tip. The organic solvent was removed under vacuum (Rotavapor, Büchi) to cause a phase inversion that gave an O/W emulsion. The obtained liposomes L, ML (magnesium containing liposomes), L-EGCG (EGCG loaded liposomes) and ML-EGCG (magnesium containing liposomes loaded with EGCG) were characterized fresh and/or after equilibration for 24 h. The liposomal suspensions containing Poloxamer-407, PxL (poloxamer liposomes), MPxL (magnesium-containing poloxamer liposomes), PxL-EGCG (poloxamer liposomes loaded with EGCG) and MPxL-EGCG (magnesium-containing poloxamer liposomes loaded with EGCG) were prepared in the same way, but Poloxamer-407 was added in PBS to obtain a polymer final concentration of 0.8 mg mL^{-1}. Note that the MLV suspensions were directly used for X-ray diffraction experiments, while samples for DLS characterization, turbidimetric analysis, encapsulation efficiency determination, *in vitro* release and cellular assays, were sonicated (sonic Vibracell) before being used for 30 min in pulse mode (30 sec on; 2 sec off, 50%) at 0 °C, until the liposome dispersion was completely clear.

X-ray diffraction

X-ray diffraction experiments were performed using a 3.5 kW Philips PW 1830 X-ray generator (Amsterdam, Netherlands) provided with a bent quartz crystal monochromator (λ = 1.54 Å) and a Guinier-type focusing camera (homemade design and construction, Ancona, Italy). Diffraction patterns were recorded on GNR Analytical Instruments Imaging Plate system (Novara, Italy). MLV suspensions were measured in a tight vacuum cylindrical cell equipped with thin mylar windows. Experiments were performed as a function of temperature, at 25, 36, 40 and 45 °C.

In each experiment a few Bragg peaks were detected. Peak indexing was performed considering the usually observed lipidic phases (Esposito et al., 2016) and the unit cell dimension of the phases, *d*, calculated from the averaged spacing of the observed peaks.

According to the decomposition of the sample in the hydrophobic and hydrophilic regions (Pabst et al., 2000), a simple equation relates the unit cell dimension to the lipid head-to-head distance, d_{HH}, that can be measured from electron density maps (Di Gregorio et al. 2010), and the thickness of the water layer d_w :

$$d_w = d - d_{HH}$$

Therefore, the area-per-lipid at the water/lipid interface S_{lip} and the averaged number of water molecules associated with one lipid molecule $n_{w/lip}$ can be determined if v_{lip} and v_{wat}, the averaged lipid molecular volume (in this case estimated by MD simulations to be around 960 Å^3) and the water molecular volume (30 Å^3) are known:

$$S_{lip} = 2v_{lip} / d_{HH}$$

and

$$n_{w/lip} = V_{w/lip} / v_{wat}$$

with $V_{w/lip} = d_w S_{lip} / 2$.

Physicochemical characterization of liposomes.

The intensity-based diameter (Z-average) and the polydispersity index (PDI) of liposomes were measured by Dynamic Light Scattering (DLS) and Electrophoretic Light Scattering using a Malvern Zetasizer Nano ZS (Malvern Instruments GmbH). An aliquot of every liposome suspension, obtained by sonication, was diluted at a final concentration of 2.5 x 10^{-2} mM with ultra-purified water. Measurements were performed at 25 °C with a fixed angle of 173°. Size particle measurements and the polydispersity index were calculated from the autocorrelation function by cumulant analysis (Dispersion Technology Software V7.11 provided by Malvern Instruments). Zeta potentials were determined by the Zetasizer software from the electrophoretic mobility applying Henry's equation

and using Smoluchowski's approximation. For all samples investigated, the data represent the average of at least three different autocorrelations carried out for each sample.

Determination of encapsulation efficiency with gel filtration method

Liposomes were separated from non-encapsulated EGCG by size exclusion chromatography. The disposable syringes **(**2.5 mL), packed with hydrated Sephadex G-25 resin were placed in 15 mL plastic test tubes. After preconditioning with PBS, 0.8 mL of EGCG-loaded liposomes were gently added on the top of the syringes and centrifuged at 500 g for 10 min. Empty liposomes and free EGCG were also used as control. The eluates were collected at the bottom of the test tubes and the Stewart assay was carried out to determine the lipid content in the liposome preparation after gel filtration. To evaluate the encapsulation efficiency, 150 μL samples of purified and unpurified liposomes were lysed by addition of Triton X-100 to a final concentration of 1% (v/v) and the complete release of the antioxidant was obtained. After lysis the EGCG concentration was estimated by the Folin-Ciocalteu assay (Liang et al., 2014). 150 μL of 10% Folin-Ciocalteu reagent was added to 50 μL of every sample into a 96-well microplate and shaken. After 10 min 0.100 mL of a 7.5% sodium carbonate solution was added and the mixtures were allowed to incubate in the dark for 1 h at room temperature for colour development. After incubation, the absorbance was measured at 765 nm on a BioTek Synergy HT MicroPlate Reader Spectrophotometer using a blank containing all the appropriate components except EGCG. The calibration curve was plotted using EGCG. The encapsulation efficiency (EE) and the drug loading capacity (DLC) were calculated using the following formulae:

$$EE\ (\%) = 100 \times [C_{int} / C_{total}]$$

$$DLC\ (\%) = 100 \times [C_{int} / C_{lipid}]$$

where C_{total} refers to the total concentration of the antioxidant measured in the unfiltered liposomes, C_{int} refers to the concentration of the encapsulated antioxidant (which was the amount of EGCG measured inside purified liposomes after lysis), and C_{lipid} is the total lipid concentration. All the experiments were repeated at least three times and measurements were run in triplicate.

***In vitro* EGCG release**

The *in vitro* antioxidant release from liposomes was studied by the dialysis method. Dialysis bags were soaked in PBS at room temperature for 2 h before use to remove the preservative, and then rinsed thoroughly in the same buffer solution. 1 mL of MPxL-EGCG (1 mM, EGCG) was placed in the dialysis bag (12,000 MW cut off; Sigma-Aldrich) and dialyzed against 10 mL of release buffer

(PBS). Control bags, containing EGCG with $MgCl_2$ were prepared and dialyzed. The dialysis process was performed under stirring at 100 rpm at 37 °C and kept away from bright light. At appropriate time intervals, 1 mL of the outer aqueous solution was withdrawn for analysis and immediately replaced by an equal volume of fresh release buffer. The cumulative amount of EGCG released was analyzed by the Folin−Ciocalteu assay as described above. The profiles of *in vitro* EGCG release from liposomes and the accumulative release percentage of catechin (RE %) was expressed according to the experimental equation:

$$RE\ \% = 100 \times (C_{0\text{-}t} / C_0)$$

Where $C_{0\text{-}t}$ is the amount of drug released from liposome suspension from the beginning to the scheduled time, and C_0 is the total amount of drug in liposome suspension. The data represent the average of at least three different analyses carried out for each sample.

Cell treatment

ARPE19 cells were routinely maintained in 25 cm^2 flasks in complete DMEM/F12 medium at 37 °C, 5% CO_2 and 95% relative humidity. Complete DMEM/F12 medium was prepared by adding 10% (v/v) heat-inactivated fetal bovine serum (FBS), 2 mM glutamine and 100 U/ml penicillin-streptomycin. Culture medium was changed every 2 days until cells grew to 90% confluence. The cell cultures were detached by trypsinization with 0.5% trypsin in PBS containing 0.025% EDTA and counted using trypan blue exclusion assay.

For treatments, ARPE19 cells were seeded in 24-well plates at 8×10^4/well to reach 50-60% of confluence at 24 h. In the cytotoxicity assay, the cells were incubated for 24 h with increasing concentrations of MPxL-EGCG and unloaded MPxL (35, 55, 75, 90 and 115 μg mL^{-1} of lipid) or free EGCG in presence or absence of magnesium salt. The free EGCG was added at concentrations equal to the EGCG content in the liposomal formulations (EGCG, 22/33/44/55/66 μM). For the cytoprotection assay, the cells were treated with DMEM/F12 only (Ctrl), 55 μM and/or 90 μg mL^{-1} of EGCG and lipid concentrations, respectively. After 24 h of incubation, the cells were washed twice with PBS and treated with 6 mM H_2O_2 for 6 h. The combination of dose/time of H_2O_2 treatments was established according to previous MTT viability assay for cytotoxicity studies (data not shown).

Assay of mitochondrial viability (MTT assay)

To evaluate the number of metabolically active cells, and thus cell viability, we used the 3-(4,5-dimethylthiazol-2-yl)-2,5-diphenyltetrazolium bromide (MTT) assay (Mosmann, 1983). At the time

of analyses, the medium from each well was removed and replaced with fresh medium supplemented with 100 µg MTT (50 µL from the 2 mg mL^{-1} stock); samples were incubated for 3 h at 37 °C in 5% CO_2 atmosphere, until formazan crystals were formed. Next, 400 µL of DMSO was added to each well and mixed thoroughly by shaking to solubilize the MTT formazan crystals. Absorbance was read on a multiwell scanning microplate reader (BioTek Synergy HT MicroPlate Reader Spectrophotometer) at 570 nm using the extraction buffer as blank. The optical density in the control group (untreated cells) was considered as 100% viability. The relative cell viability (%) was calculated as (A570 of treated samples/ A570 of untreated samples) x 100. Each experiment was performed at least five times in triplicate.

Transmission Electron Microscopy (TEM)

ARPE19 cells were plated on Aclar films (Ted Pella CA, USA) for flat embedding and were treated as in the cytoprotection assay. After H_2O_2-treatment the cells were fixed for 1 hat room temperature (rt) with a solution of 2.5 Glutaraldeyde in 0.1 M cacodylate buffer (pH 7.4) then post fixed in 1% osmium tetroxide in 0.1 M cacodylate buffer for 30 min at rt followed by dehydration in acetone series and embedded in epoxy resin (Sigma #43359). Ultrathin (40 nm) section were stained with lead citrate and uranyl acetate and imaged on a Philips CM12 TEM at 100 KV. Images were digitally captured using Olympus Veleta or Megaview G2 digital camera that were previously calibrated for every magnification used.

Qualitative evaluation of cell morphology was done considering the normal cell morphology of nucleous, nuclear membrane, endoplasmic reticulum, mitochondria and villi (Kamogashira, 2017).

Statistical analysis

Data are presented as mean ± S.D. Statistical comparison of differences among groups of data was carried out using Student's t-test. p-values ≤ 0.05 were considered statistically significant, p-values ≤ 0.01 and p-values ≤ 0.001 were considered highly significant.

Results and Discussion

1. Liposome formulation: effect of Poloxamer-407 addition.

EGCG shows a remarkable antioxidant activity, but its chemical and metabolic instability determines a low concentration of the antioxidant within the biological system after administration. In previous studies, we showed that full EGCG encapsulation in both anionic and neutral liposomes can be obtained by salt addition (Torchilin, 2005; Nakayama et al., 2000). In particular, we found that anionic

multilamellar vesicles (MLV) prepared with POPC/DOPE/CHEMS (**Figure 2**) in equimolar ratio (1:1:1) maximize the encapsulation of EGCG in the presence of magnesium salt. The choice of such a mixed liposome composition takes advantage of DOPE's ability to fuse with cell membranes (Huth et al., 2006), while CHEMS, a cholesterol synthetic derivate with a negative charge, creates an anionic environment**.** Furthermore, the cholesterol moiety confers high stability to the bilayer: its ability in increasing the packing of the phospholipid component of liposomes and reducing the bilayer permeability to solutes is in fact well-known (Papahadjopoulos et al., 1973).

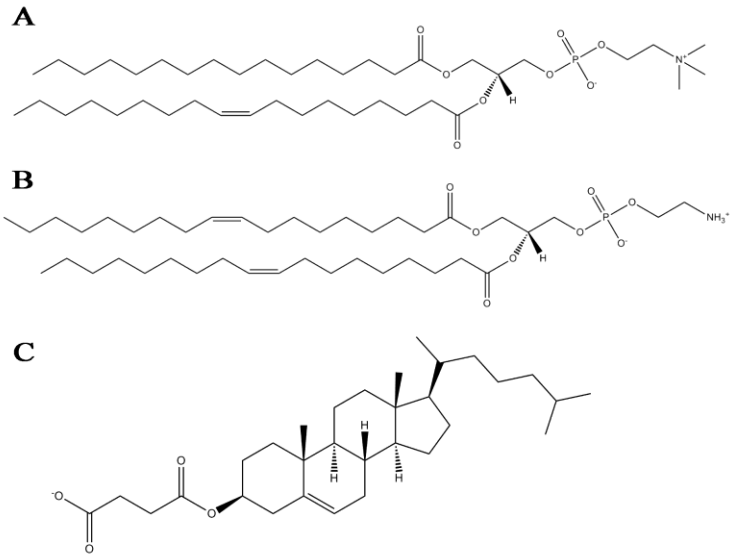

Figure 2. 2D structure of POPC (A), DOPE (B) and CHEMS (C)

With the aim to obtain an efficient antioxidant liposomal system, we optimized the best anionic formulation to achieve a stable nanodispersed suspension suitable for drug delivery applications. Indeed, complete encapsulation was observed with an equimolar lipid ratio POPC/DOPE/CHEMS (final lipid concentration 3 mg mL^{-1}) containing 460 μg mL^{-1} of EGCG and magnesium salt at 5:1 $MgCl_2$/EGCG molar ratio. However, as reported in **Figure 3**, although the simultaneous presence of EGCG and magnesium salts, had maximized the EGCG encapsulation, it induced an increase in particle size, followed by cluster aggregate's formation which are visible to the naked eye. The high encapsulation of EGCG achieved and the presence of magnesium seem to be responsible for the physical instability of the liposome suspension in terms of aggregation/flocculation, probably due to the presence of numerous hydrogen bond donors in the EGCG structure and to its metal chelating properties. The turbidimetric measurement of ML systems demonstrated that magnesium promotes the formation of large particles but not of precipitates, whereas L-EGCG suspension, containing only

the polyphenol, showed a turbidimetric value slightly lower than empty liposomes. Every attempt to obtain a stable suspension of ML-EGCG nanosized particles failed; DLS measurements carried out after sonication showed the presence of a polydispersed system (size 345 ± 43.97 nm, PDI 0.503 ± 0.041) that tends to aggregate in the following 24 h and gives particles larger than 2 μm.

In light of the well-known properties of several surfactants that drastically increase the stability of lipid dispersion and prevent their aggregation (Hsu and Nacu, 2003) we added Poloxamer-407 to the non-homogeneous suspension of liposomes until the agglomerates were efficiently resuspended as shown in **Figure 3** where turbidity data for L, ML, L-EGCG, ML-EGCG and MPxL-EGCG are reported. The presence of the polymer seems to influence the interaction between liposomes and gives rise to an opalescent homogeneous suspension demonstrating that the Poloxamer-407 is able to hinder liposomes aggregation probably by shielding the colloidal surface with the hydrophilic portions of the polymer. The final concentration of Poloxamer-407 necessary to obtain a homogeneous suspension was 0.8 mg mL^{-1}.

A

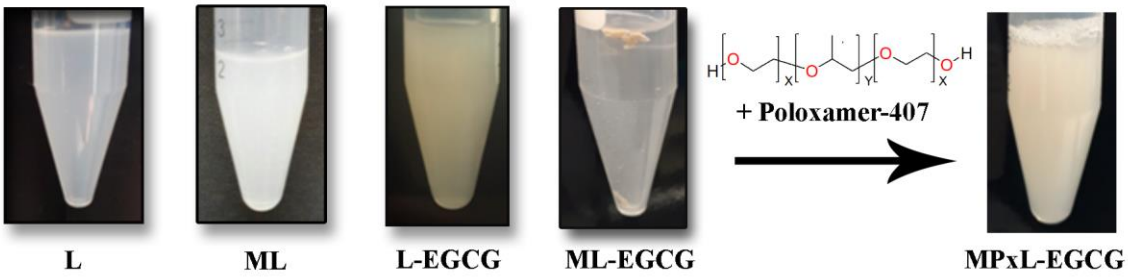

B

	L	*ML*	*L-EGCG*	*ML-EGCG*	*MPxL-EGCG*
OD (λ, 500 nm)	0.700 ± 0.167	1.215 ± 0.098	0.558 ± 0.098	0.069 ± 0.025	0.658 ± 0.025

Figure 3. Aggregation induced by EGCG and magnesium salt. A) Photography of MLV liposomes in the presence of only magnesium salt and EGCG alone or their combination. Stabilizing effect achieved in presence of 0.8 mg ml^{-1} Poloxamer-407. **B)** Optical density (OD) at 500 nm of all MLV suspensions studied.

2. Characterization of bulk and nanodispersed liposomal phase

2.1 X-ray diffraction measurements

To analyze the structure of the MLVs and the influence of EGCG and magnesium cations on the supramolecular properties of the self-assembled nanoparticles, X-ray diffraction experiments were carried out on L, ML, L-EGCG and ML-EGCG systems, prepared both in the absence and in the presence of Poloxamer-407.

The X-ray diffraction profiles obtained in the absence of Poloxamer-407 are reported in **Figure 4**.

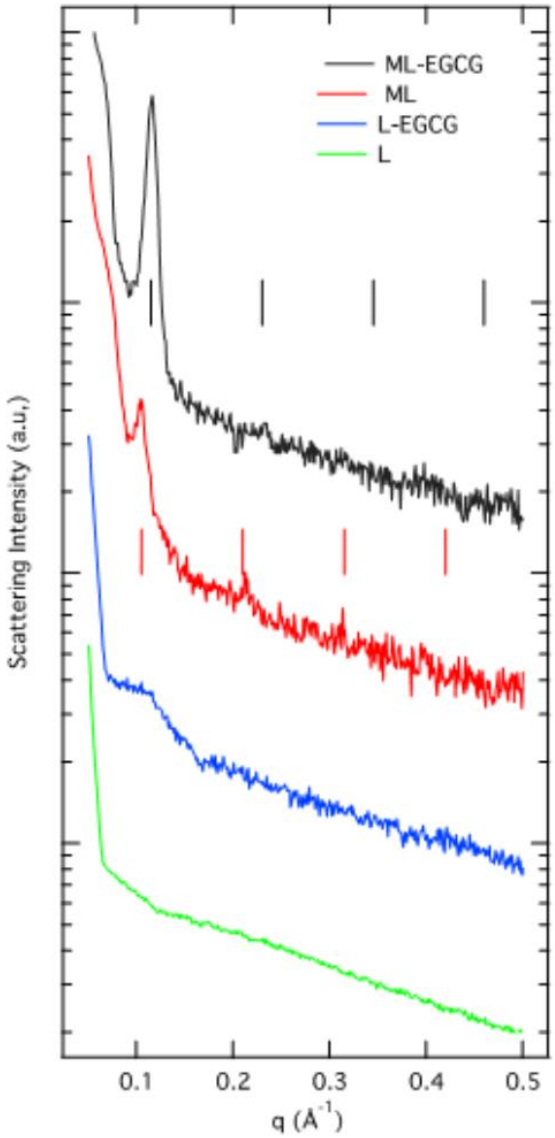

Figure 4: X-ray diffraction profiles from L, ML, ML-EGCG, L-EGCG systems. The temperature was 25 °C.

Depending on composition, different characteristics are observed: for L and L-EGCG samples, a very large band (centered at about 57 Å) occurs in the low-*Q* region, suggesting the formation of a disordered system, probably unordered MLVs or LUVs; on the other side, 3 or 4 Bragg peaks characterize the diffraction profiles of ML and ML-EGCG samples, indicating that the presence of Mg^{2+} induces the formation of a rather ordered structure. As the peak spacing ratios scale as 1:2:3..., a 1-D lamellar organization is proposed: the well-known rearrangement of the lipidic carbonyl region (Binder and Zschörnig, 2002), which accompanies Mg^{2+} binding and which involves hydration and conformational changes, appears to stabilize the lamellar structure, even in the presence of EGCG. ML and ML-EGCG samples then show the same multilamellar structure, the main difference being the unit cell dimension (e.g., the repeat distance among the lamellae, *d*), which is larger for ML (59.8

± 0.5 Å) and smaller for ML-EGCG (54.6 ± 0.5 Å). The 10% reduction observed in the presence of EGCG can be related to a different lipid hydration induced by the presence of the active molecule or to changes in the hydrocarbon chain conformation, which is more disordered when EGCG is present. To disentangle the different structural effects, low-resolution electron density profiles have been calculated, as reported by Di Gregorio et al. (Di Gregorio et al., 2010). Electron density maps, reported in **Figure 5**, show small differences in the position of the maxima corresponding to the head-group location and in the form of the electron density in the hydrocarbon region (see the differences between the full and the dashed lines).

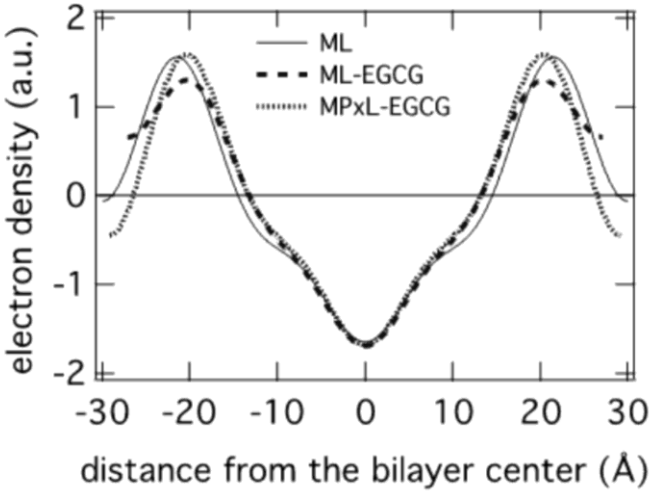

Figure 5. Reconstructed electron density profiles for the lamellar phase of ML (full line), ML-EGCG (dashed line) and MPxL-EGCG (dotted line) systems at 25 °C.

From the head-to-head electron density peak distance, the lipid bilayer thickness was obtained and, according to the decomposition of the sample in the hydrophobic and hydrophilic regions (Pabst t al., 2000), the average lipid cross sectional area, S_{lip}, and the lipid-associated intermembrane water volume, $V_{w,lip}$, were derived using equations reported in the *Material and Methods* section.

Table 1. Structural and molecular parameters for ML, ML-EGCG and MPxL-EGCG

System	***d*** **(Å)**	d_{HH} **(Å)**	d_{wat} **(Å)**	S_{lip} **(Å^2)**	$V_{w/lip}$ **(Å^3)**	$n_{w/lip}$
ML	59.8	44	15.8	43.6	345	11
ML-EGCG	54.6	40	14.6	48.0	350	12
MPxL-EGCG	58.1	40	18.2	48.0	436	-

The results shown in **Table 1** are compatible with the location of EGCG near the lipid head-group, so as to induce an increase in the area-per-lipid at the polar/apolar interface and an increased disorder of the lipid hydrocarbon chains. Of note is that hydration is not modified, as indicated by the rather constant lipid-associated intermembrane water volume (e.g., the number of water molecule-per-lipid is practically the same); consequently the formation of aggregates has to be ascribed to the strong interaction between EGCG and lipid-head group rather than to dehydration phenomena.

This result can be related to the high encapsulation efficiency observed in our liposomal system but also to the occurrence of precipitates in the liposome formulation containing both Mg^{2+} and EGCG. Indeed, the interaction network is complex. On the one hand, EGCG can behave both as H-donor with lipid oxygen groups and as H-acceptor with ethanolamine groups in DOPE; on the other hand, the presence of magnesium ions enhances the interaction possibilities between EGCG and the lipid bilayer. In fact, at physiological pH, EGCG is partially deprotonated (its pKa is 7.75) so that magnesium divalent ions can serve as cross-bridge to bind phosphate or oxygen lipid groups. Moreover, the presence of CHEMS, which is a negatively charged steroid molecule, increases the electrostatic interactions with Mg^{2+} ions, indirectly promoting the interaction of EGCG with the lipid bilayer (Laudadio et al., 2018).

X-ray diffraction profiles related to samples prepared in the presence or absence of Poloxamer-407 were very similar. **Figure 6** shows the results obtained from ML-EGCG and MPxL-EGCG carriers as a function of temperature: in both cases the multilamellar structure is confirmed by the Bragg peak sequence. Furthermore, the peak reciprocal intensities are maintained even at 45 °C, so guaranteeing the antioxidant liposome stability at physiological temperature.

If the two carriers show the same structural stability on heating, the polymer has an ordering effect on the supramolecular organization of liposomes and induces a change in the unit cell, which increases from 54.6 to about 58 Å. According to the unit cell temperature dependence reported in **Figure 6**, such an increase is probably determined by the presence of polymer molecules in between the lipid layers. In fact, as reported elsewhere (Djekic et al., 2015), Poloxamer-407 has two water-soluble PEO chains and a more hydrophobic middle block that may be adsorbed at, or incorporated in, the surface of the lipidic structural elements. As a consequence, steric repulsion between bilayers could occur.

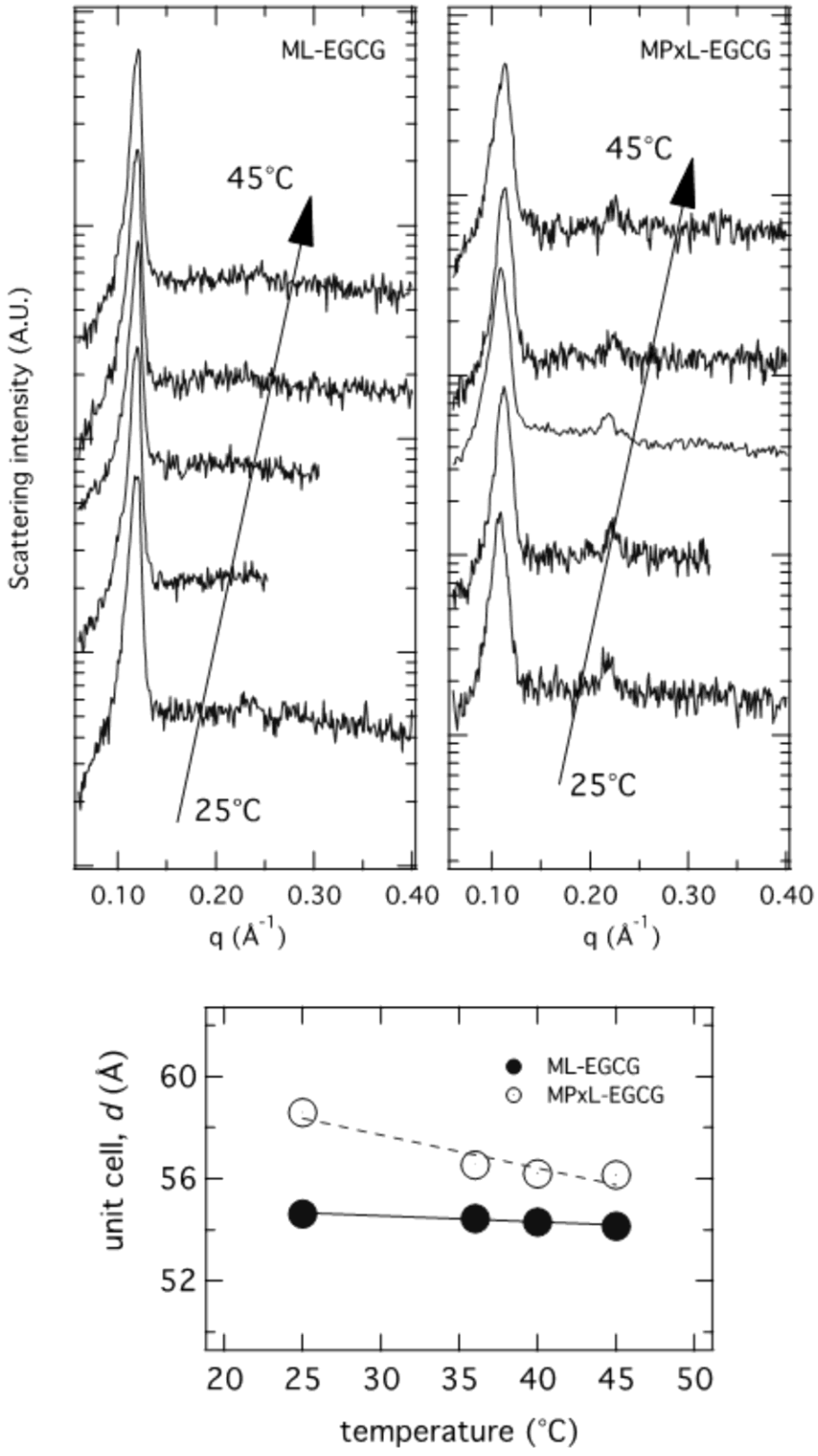

Figure 6. X-ray diffraction profiles observed for ML-EGCG (left frame) and MPxL-EGCG (right frame) samples as a function of temperature, as indicated. The lower frame shows the temperature-dependence of the lamellar repeat distance, as determined from the analysis of the position of the observed Bragg peaks.

Electron density maps confirm this view: the profiles calculated at 25 °C for ML-EGCG and MPxL-EGCG samples, and reported in **Figure 5** (compare the dashed and the dotted lines), show that the head-to-head electron density peak distance is practically unaltered by the presence of Poloxamer-407 (hence, no changes in lipid conformation and in average lipid cross sectional area are expected). Moreover, while the inner lamellar part shows very similar features, differences are observed in correspondence of the polar region. Poloxamer-407 does not affect the lipid packing, but steric effects due to adsorption at the polar-head region enlarge the lamellar repeat distance (note the consequent increases of the lipid-associated intermembrane volume, referred as $V_{w,lip}$, in Table 1).

In order to verify the time stability, structural studies were also performed on MPxL-EGCG samples after storage at 4 °C for 1 month: X-ray diffraction profiles confirm that the inner multilamellar morphology is preserved, with a very small reduction of the unit cell dimension to 57.1 Å, well inside the experimental error (estimated around 0.5 Å).

2.3 Dynamic Light Scattering

All the liposomal formulations were sonicated after addition of Poloxamer-407 and measurements of size distribution and zeta potential were carried out. As shown in **Table 2**, the presence of Poloxamer 407 confers high stability to all the suspensions and prevents aggregation; the intensity mean diameter of MPxL-EGCG, expressed as *Z* average, was about 205 nm with a certain degree of polydispersity (PDI about 0.3) and the size did not change after 24 h. The analysis per number revealed that the most representative amount of vesicles displayed a mean diameter of 140 nm; a bimodal distribution was highlighted by the intensity and volume based particle size distribution where an additional population of about 370 nm was present. The DLS measurements did not show the presence of micelles. The stability of MPxL-EGCG stored at 4 °C was also evaluated after 1 month. The intensity-based distribution evidentiated the presence of some amounts of aggregates of 0.8-1.0 µm, which are not present in the number-based distribution where the only peak corresponds to a population of about 150 nm. The negative zeta potential of liposomes due to the presence of CHEMS decreased in absolute value in the presence of Mg^{2+} because of the absorption of positive ions; in MPxL-EGCG, the zeta potential is further reduced: the ability of EGCG to chelate positive ions is probably responsible for a major absorption of magnesium ion on the liposome surface. By virtue of the presence of Poloxamer-407, the EGCG magnesium liposomes did not aggregate in spite of their low zeta potential.

Table 2. Characterization of sonicated liposomes with Poloxamer-407 [a,b]

Liposomes Formulation	Time of analyses (h)	Particle size ± SD (nm)	PDI ± SD (nm)	ζ-potential ± SD (mV)	Encapsulation Efficiency (EE%)	Loading Capacirty (LD%)
PxL	0	99.8 ± 11.9	0.221 ± 0.004	-40.0 ± 0.2	n.a	n.a.
	24	137.0 ± 12.5	0.268 ± 0.048			
MPxL	0	112.8 ± 6.4	0.329 ± 0.047	-29.5 ± 3.5	n.a	n.a.
	24	123.5 ± 4.2	0.282 ± 0.006			
PxL-EGCG	0	101.2 ± 13.4	0.396 ± 0.008	-43.0 ± 1.9	57.0 ± 4.5	9.2± 2.1
	24	117.4 ± 3.3	0.251 ± 0.025			
MPxL-EGCG	0	205.2 ± 8.9	0.271 ± 0.023	-17.6 ± 4.1	95.0 ± 4.8	15.0 ± 2.3
	24	201.9 ± 9.4	0.245 ± 0.015			

[a] Particle size, PDI and zeta potential were determined by DLS. Encapsulation Efficiency and Loading Capacity were determined as reported in Materials and Methods section. [b] SD: standard deviation.

2.4. Entrapment efficiency of liposomes

The percentage of EGCG encapsulated inside liposomes (PxL-EGCG and MPxL-EGCG) was determined by the Folin-Ciocalteu assay and the results are presented in **Table 2**. For the PxL-EGCG we obtained 57.0 ± 4.5 % of encapsulation efficiency, thus confirming the capacity of EGCG to form phytosomes (Galeazzi et al. 2015; Nakayama et al., 2000). Instead, in the presence of the magnesium salt, we practically reached a complete encapsulation of EGCG (95.0 ± 4.8 %), which decreased by 17 % after storage at 4 °C for 1 month. In **Table 2** the Loading Capacity of both formulations are also reported. These data confirm previous results in which $MgCl_2$ can greatly improve the interaction of EGCG molecules with anionic liposomes (Laudadio et al., 2018) and consequently we chose the anionic formulation MPxL-EGCG, presenting the best encapsulation outcome, for the following experiments.

2.5. *In-vitro* drug release

I*n-vitro* antioxidant release from MPxL-EGCG was evaluated by dialysis method at 37 °C in PBS and the results, compared with free EGCG behavior, are presented in **Figure 7** as cumulative percentage release during 24 h.

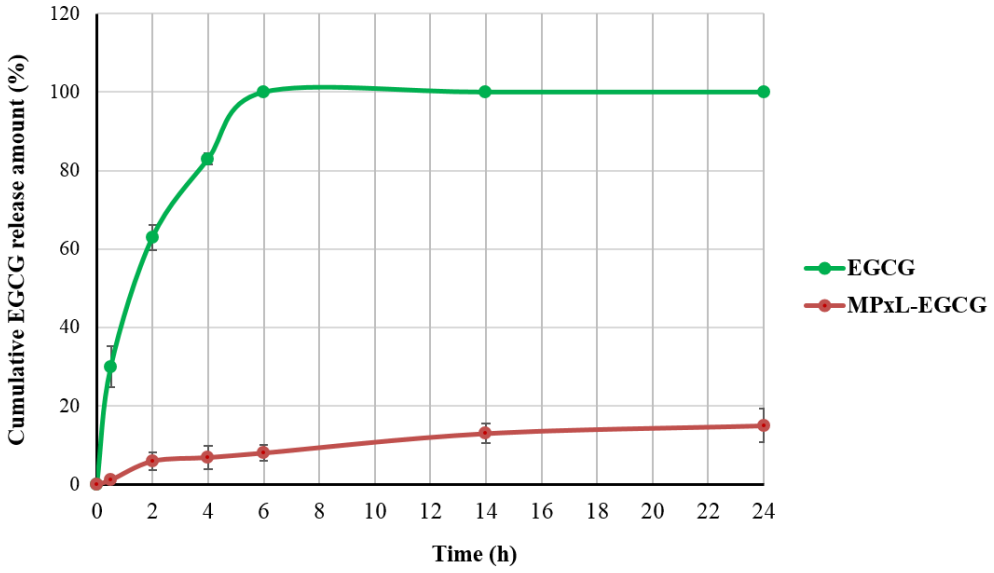

Figure 7. *In vitro* release of EGCG in PBS (pH 7.4) for liposomal and free drug solution. Values are expressed as mean ± SD; n=3 independent experiments.

The diffusion of free antioxidant through the dialysis membrane from the control was more than 60% in the first 2 h and complete by 6 h, demonstrating that the dialysis membrane did not limit the release of EGCG. The drug encapsulation in liposomes modified its release profile: the MPxL-EGCG release was about 6 % in the first 2 h and reached 15% after 24 h. Evidently, the strong interaction underlined *in silico* (Laudadio et al., 2018) between anionic liposomes and EGCG in the presence of magnesium ions determines the low release of the molecule from liposomes. The presence of Poloxamer-407 on the liposomal surface can contribute to reduce the speed of release of encapsulated EGCG.

2.6. Stability of magnesium poloxamer-liposomes formulation in serum

The physical stability of the produced liposomes was studied in the presence of plasma proteins, after their exposure to serum, using DLS and turbidity measurements. For this purpose, liposomes were incubated in PBS supplemented with FBS (50% v/v) at 37 °C and measurements were carried out at 0 and 24 h.

For both MPxL and MPxL-EGCG dispersion, the average dispersed vesicle diameter remained essentially unchanged upon exposure to 50% FBS (t=0), even after 24 h (**Table 3**).

.

Table 3. Influence of serum on size distribution of Magnesium Liposomes with Poloxamer-407[a,b].

Liposomes Formulations	Time of analyses (h)	Size in serum ± SD (nm)	λ=500 nm		λ=600 nm	
			Serum	PBS	Serum	PBS
MPxL	0	106.3 ± 12	0.086	0.068	0.082	0.066
	24	90.65 ± 14	0.085	0.067	0.081	0.066
MPxL-EGCG	0	210.9 ± 7.4	0.124	0.103	0.108	0.090
	24	189.2 ± 9.1	0.134	0.103	0.116	0.092

[a] Particle size was determined by DLS. Turbidity of the dispersions was determined as OD as reported in Materials and Methods section. [b] SD: standard deviation; PBS: phosphate buffered saline.

We confirmed the liposomal suspension stability by spectroturbidimetry. Because the absorbance is considerably affected by the change in size of particles (; Minami et al., 1999), this technique can be used to reveal the instability of a colloidal suspension due to the aggregation of vesicles and for diluted suspension of vesicles with small refractive index, the turbidity and the optical density are proportional to the scattered light. The optical densities at 600 and 500 nm for particles in PBS and in 50% of FBS are reported in **Table 3**. At these wavelengths, the absorbance for the liposomes in serum, as well as in PBS, increased only slightly or nothing with time, indicating that the dispersions are stable as highlighted from DLS results.

3. Cellular experiments

Once the structural and stability properties of EGCG-loaded nanoparticles were determined, cellular experiments were performed to assess cytotoxicity and potential activity as antioxidant delivery system.

3.1. Cytotoxicity of EGCG-loaded magnesium-poloxamer liposomes in Retinal Pigment Epithelial Cells

The toxicity of MPxL-EGCG was evaluated in ARPE-19 cells by MTT assay and compared with that of corresponding concentrations of free EGCG (**Figure 8**). To exclude both positive and negative Mg^{2+} effect on cells vitality, we tested the EGCG molecule with and without magnesium ions. Moreover, unloaded MPxL were also tested to verify the potential toxicity of the lipid vector used in the present study.

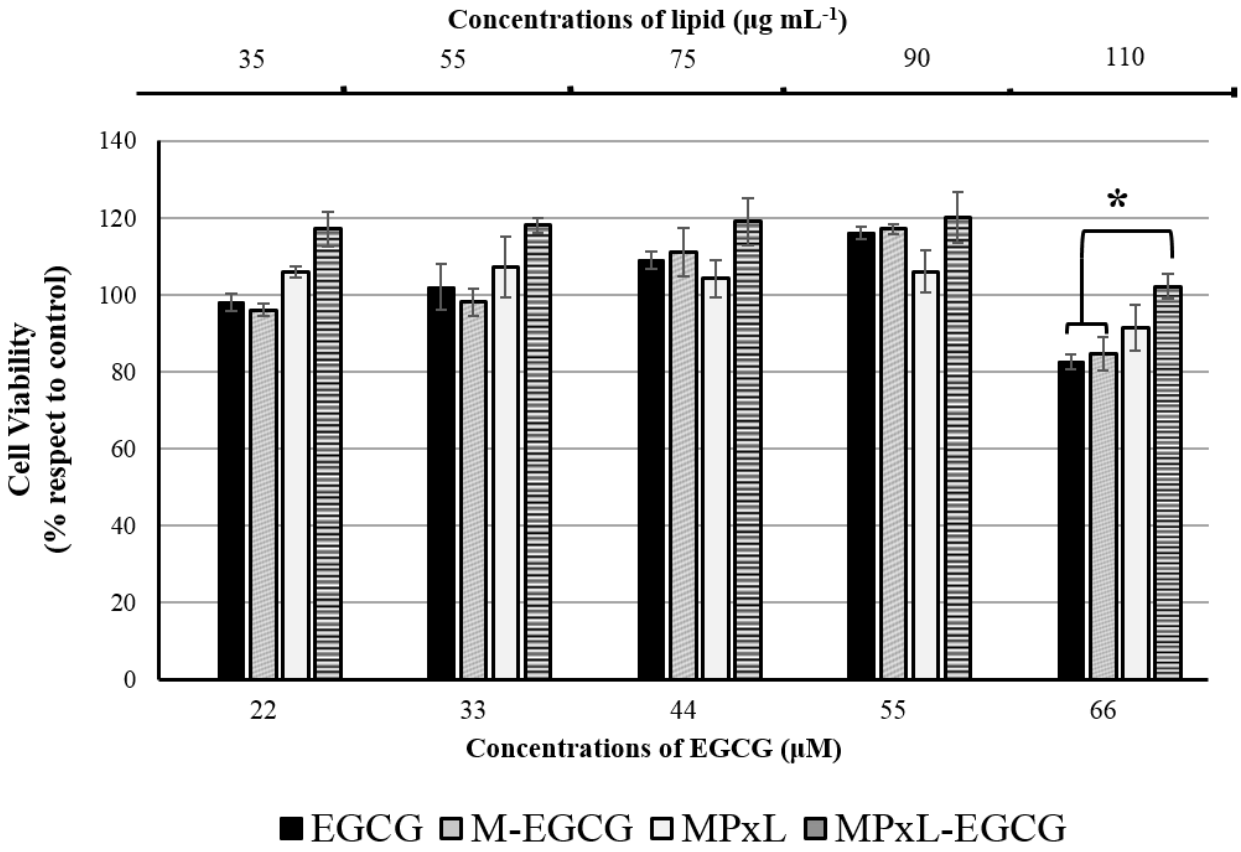

Figure 8. Cytotoxicity of free and encapsulated EGCG liposomes in ARPE19 cells. The cells were treated with various concentrations of MPxL-EGCG, MPxL, EGCG, and M-EGCG (at concentrations equal to the catechin content in the liposomal formulations) for 24 h in complete culture medium. The respective concentration of lipid (µg mL^{-1}) for each EGCG concentration tested in liposomes is reported above the histogram. Cell viability was determined by MTT assay. The values in the figures are expressed as the means ± SD. Significant differences can be observed between cell viability in the presence of MPxL-EGCG vs. EGCG and M-EGCG groups, at 66 µM and 110 µg mL^{-1} of catechin and lipid, respectively (*$p<0.05$).

The free EGCG shows low cytotoxicity in ARPE-19 cells. In detail, EGCG treatment did not decrease cell viability up to 55 µM (**Figure 8**); at this percentage we observed instead an increase in viable cells in relation to the control (55 µM, 115%). At 66 µM EGCG concentration, we observed ca. 20% decrease in cell viability probably due to the pro-oxidative action of molecules at high concentrations (Li et al., 2010) and/or to its strong interaction with cellular membranes (Nakayama et al., 2000) leading to membrane leakage, change in membrane potential, and increase in permeability to protons and potassium ions (Caturla et al., 2003). The same result was obtained with EGCG in presence of magnesium ions, thus demonstrating that the bivalent salt concentrations, used in this study, did not affect cell viability (**Figure 8**). Empty liposomes showed a similar trand as free EGCG with a decrease in cell survival only at high concentration of lipid (110 µg ml^{-1}, ca. 20% of cell death compared to

no-treated cells). In the MPxL-EGCG-treated cells, no decrease in cell viability compared to the control was observed at the highest concentration of EGCG and lipid, despite an overall drop compared to lower concentrations. The employment of liposomes probably allows EGCG internalization thus avoiding massive surface membrane interactions that can alter cell membrane fluidity and permeability. Based on these results, we chose the 55 μM concentration of bioactive molecule which corresponds to 90 μg mL^{-1} of lipids for the experiments described in the next section.

3.2. Enhancement of EGCG efficacy by magnesium-poloxamer liposome incorporation

In order to study MPxL-EGCG potential ability to protect ARPE-19 cells from physiological stressors, oxidative damage mediated by hydrogen peroxide was induced. (Iloki-Assanga et al., 2015). MPxL-EGCG activity was compared with that of free EGCG and empty liposomes; in particular we examined both inhibition of oxidative stress-induced cell death and morphological changes that occur in the cytoplasm, mitochondria and nucleus of cells (**Figure 9**). After pre-treatment of ARPE-19 with EGCG alone, MPxL and MPxL-EGCG for 24 h, cells were washed twice with PBS to avoid direct extracellular interactions between the tested compounds and the oxidant. As shown in **Figure 9A**, the free EGCG treatment, as described above, effectively protects ARPE19 cells from H_2O_2-induced cell death (15% more cell viability than H_2O_2-exposed cells, $p<0.05$). The results also reveal that empty liposomes MPxL had a protective effect against H_2O_2-induced cell death (12% more cell viability than than H_2O_2-treatedcells, $p<0.05$); lipids play in fact an important role in cellular regulation, as building blocks of membranes but also in transducing intra- or extracellular signals. Consequently, liposomes can have a positive influence on cellular viability and appear suitable for drug delivery application. (Caddeo et al., 2008) The encapsulation of EGCG in magnesium liposomes markedly enhanced their protective effect against oxidative stress with an increase in cell survival of 40% compared to H_2O_2-exposed group cells ($p<0.001$) and up to 25-28% when compared to free EGCG and empty liposomes, respectively (**Fig.9A**).

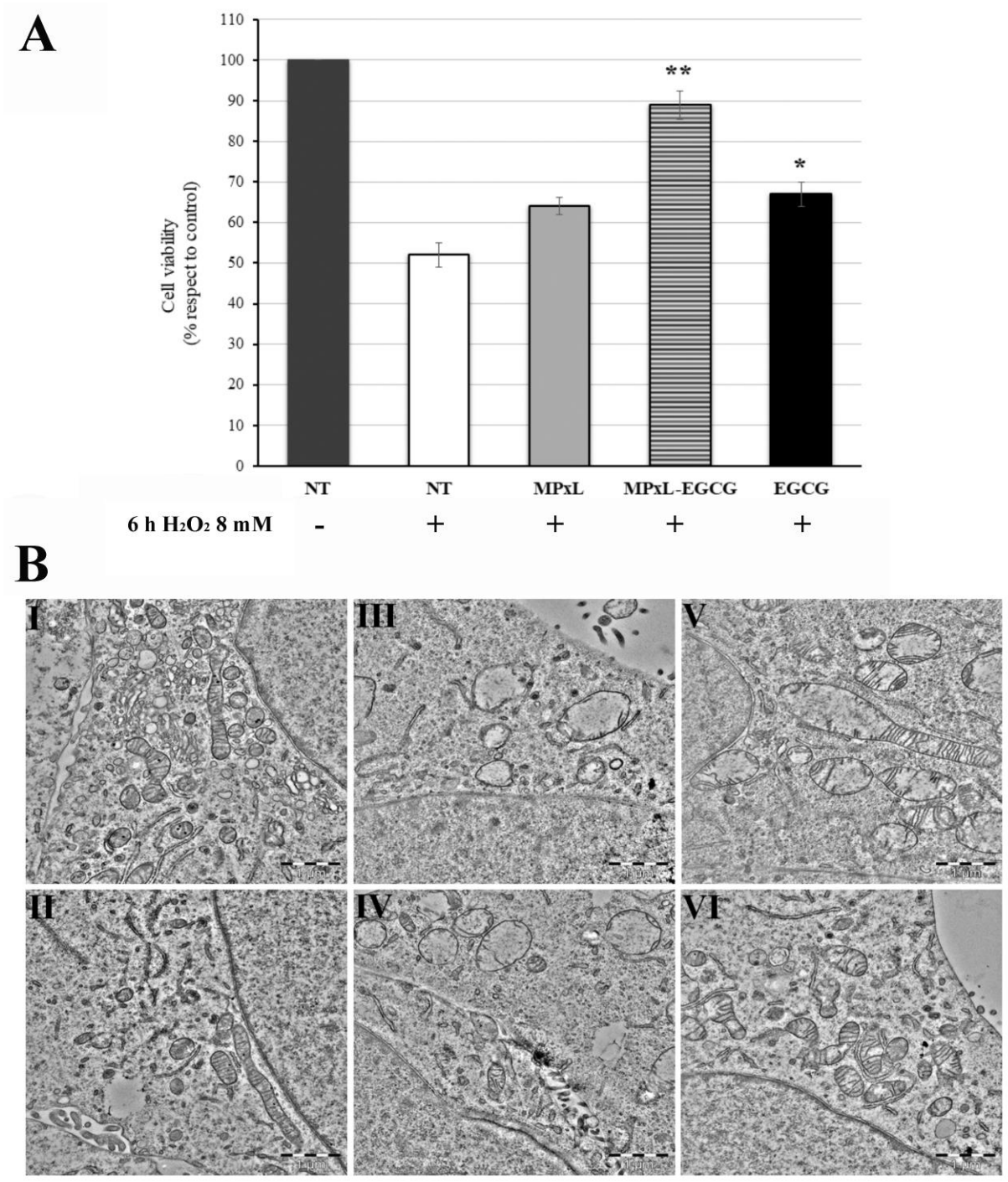

Figure 9. Effect of free EGCG and EGCG loaded in magnesium-poloxamer liposomes in ARPE19 cells after H_2O_2 exposure. The cells were pre-treated with 55µM free EGCG or EGCG encapsulated in MPxL, which correspond to 90 µg mL^{-1} lipid for 24 h, before being exposed to 6 mM H_2O_2 for 6 h. **A)** Cell viability was determined by MTT assay. Data are expressed as means ± S.D. of five independent experiments, each performed in triplicate, **$p < 0.001$, *$p < 0.05$ difference from control, representing cells treated only with H_2O_2.; **B)** Qualitative evaluation of cell morphology was done by TEM analyses. I, II: Control cells with normal mitochondria, nuclear membrane, Golgi, striated endoplasmic reticulum and villies between cells. III: H_2O_2,treated cells with mitochondria bearing no cristae, swollen nuclear

membranes, fragmented reticulm with loss of ribosomes; IV: EGCG plus H_2O_2 treated cells, some mitochondria retain some cristae, reticulum retain some ribosomes; V: MPxL plus H_2O_2 treated cells, similar to III; VI. MPxL-EGCG plus H_2O_2 treated cells, many mitochondria retain cristae, a few normal ones observed, normal nuclear membrane.

We also examined, for all samples studied, ultrastructural changes of the mitochondria and other cellular features using TEM and the results are shown in **Fig. 9B**. The control group cells exhibited healthy normal appearing mitochondria, endoplasmic reticulum, presence of villi and normal nuclear membrane (**Fig. 9B, I-II)**. In contrast, H_2O_2-exposed group cells (**III**) and EGCG plus H_2O_2 group cells (**IV**) had almost completely damaged mitochondria and loss of ribosome from endoplasmic reticulum. Nuclear membrane appeared swollen and villi severely reduced. In the empty liposomes plus H_2O_2 cell group (**V**) the phenotype was less severe than in **III** and **IV** but still the nuclear membrane and mitochondria showed major morphological alterations. In the MPxL-EGCG plus H_2O_2 group cells (**VI**) the nuclear membrane appeared normal; likewise for the untreated cell, the endoplasmic reticulum was, in close proximity with mitochondria that were frequently undamaged. Overall the damage induced by H_2O_2 treatment induced substantial necrosis. Indeed, it is reported that H_2O_2 altered membranes as well mitochondria resulting in oncosis and blebbing, as defined by Majno and Joris (Majno and Joris, 1995). Moreover, we rarely observed aspects of apoptosis in all samples, suggesting that the oxidative insult was far too intense for the cells to trigger that pathway. Thus, our findings of better preserved mitochondria in the MPxL-EGCG treated cells clearly suggests that the liposomes can effectively increase the efficacy of EGCG treatment, maintaining mitochondrial integrity and vitality.

Conclusion

The development of delivery nanosystems that can improve the biological profile of an active ingredient is of utmost importance. In this work, EGCG was successfully encapsulated inside anionic liposomes in the presence of magnesium ions; we obtained complete encapsulation using liposomes prepared with an equimolar ternary lipid mixture (POPC/DOPE/CHEMS, final lipid concentration 3 mg mL^{-1}) containing 460 μg mL^{-1} of EGCG and magnesium salt at 5:1 Mg^{2+}/EGCG molar ratio. Poloxamer-407 was added to obtain stable nanodispersions, as demonstrated by DLS and turbidimetric analysis, also in the presence of serum. XRD experiments show the location of EGCG near the lipid head-group and a more ordered lamellar structure obtained by incorporation of Poloxamer-407. Because age-related macular degeneration is also caused by oxidative stress, the ability of the new liposomal system in contrasting H_2O_2-induced cell death was studied. MPxL-EGCG liposomes show superior antioxidant activity compared with free EGCG, as evaluated by MTT assay. Morphological analysis performed by TEM showed better preserved mitochondria in the

MPxL-EGCG treated cells, suggesting that encapsulated EGCG actually results very effective inside cells.

References

Binder, H.; Zschörnig, O. The effect of metal cations on the phase behavior and hydration characteristics of phospholipid membranes. *Chem. Phys. Lipids.* **2002**, *115* (1-2), 39-61.

Caddeo, C.; Teskac, K.; Sinico, C.; Kristl, J. Effect of resveratrol incorporated in liposomes on proliferation and UV-B protection of cells. *Int. J. Pharm.* **2008**, *363* (1-2), 183-91.

Caturla, N.; Vera-Samper, E.; Villalain, J.; Mateo, C. R.; Micol, V. The relationship between the antioxidant and the antibacterial properties of galloylated catechins and the structure of phospholipid model membranes. *Free Radical Biol. Med.* **2003**, *34* (6), 648–662.

Chen, Z., Zhu, Q. Y., Tsang, D., Huang, Y. Degradation of green tea catechins in tea drinks, *J. Agric. Food Chem.* **2001**, *49*, 477–82.

Crucianelli, E.; Bruni, P.; Frontini, A.; Massaccesi, L.; Pisani, M.; Smorlesi, A.; Mobbili, G. Liposomes containing mannose-6-phosphatecholesteryl conjugates for lysosome-specific delivery, *RSC Adv.* **2014**, *4*(102), 58204-7.

Di Gregorio, G. M.; Ferraris, P.; Mariani, P. Wetting properties of dioleoyl-phosphatidyl-choline bilayers in the presence of trehalose: an X-ray diffraction study. *Chem. Phys. Lipids*. **2010**, *163* (6), 601-6.

Djekic. L.; Krajisnik, D.; Martinovic, M.; Djordjevic, D.; Primorac, M. Characterization of gelation process and drug release profile of thermosensitive liquid lecithin/poloxamer 407 based gels as carriers for percutaneous delivery of ibuprofen. *Pharm.* **2015,** *490* (1), 180-189.

Dumortier, G.; Grossiord, J. L.; Agnely, F.; Chaumeil, J. C. A review of poloxamer 407 pharmaceutical and pharmacological characteristics. *Pharm. Res.* **2006,** *23* (12), 2709-28.

Esposito, E.; Mariani, P.; Drechsler, M.; Cortesi, R. Structural Studies of Lipid-Based Nanosystems for Drug Delivery: X-ray Diffraction (XRD) and Cryogenic Transmission Electron Microscopy (Cryo-TEM). In *Handbook of Nanoparticles*; Aliofkhazraei, M.; Eds.; Springer International Publishing: Switzerland, **2016**; pp 861-889.

Frei, B.; Higdon, J. V. Antioxidant activity of tea polyphenols in vivo: evidence from animal studies. *J. Nutr*. **2003**, *133* (10), 3275S-84S.

Fu, N.; Zhou, Z.; Jones, T. B.; Tan, T. T.; Wu, W. D.; Lin, S. X.; Chen, X. D.; Chan, P. P. Production of monodisperse epigallocatechin gallate (EGCG) microparticles by spray drying for high antioxidant activity retention. *Int. J. Pharm.* **2011**, *413* (1-2), 155-166.

Galeazzi, R.; Bruni, P.; Crucianelli, E.; Laudadio, E.; Marini, M.; Massaccesi, L.; Mobbili, G.; Pisani, M.; Liposome-based gene delivery systems containing a steroid derivative: computational and small angle X-ray diffraction study, *RSC Adv*., **2015**, *5*, 54070.

Gil-del Valle, L.; Gravier Hernández, R.; Delgado-Roche, L.; León Fernández, O. S. Oxidative Stress in the Aging Process: Fundamental Aspects and New Insights. In "Oxidative Stress: Diagnostics, Prevention, and Therapy", Chapter: 6; Hepel et. al.; Eds.; American Chemical Society, 2015, 6 (2), pp 177-219.

Granja, A.; Frias, I.; Neves, A. R.; Pinheiro, M.; Reis, S. Therapeutic Potential of Epigallocatechin Gallate Nanodelivery Systems. *Biomed. Res. Int.* **2017**, *2017*, 5813793.

Heitzer, T.; Schlinzig, T.; Krohn, K.; Meinertz, T.; Munzel, T. Endothelial dysfunction, oxidative stress, and risk of cardiovascular events in patients with coronary artery disease. *Circulation*. **2001**, *104*, 2673–2678.

Hernández-Zimbrón, L. F.; Zamora-Alvarado, R.; Ochoa-De la Paz, L.; Velez-Montoya, R.; Zenteno, E.; Gulias-Cañizo, R.; Quiroz-Mercado, H.; Gonzalez-Salinas, R. Age-Related Macular Degeneration: New Paradigms for Treatment and Management of AMD. *Oxid. Med. Cell. Longev*. **2018**, *1*, 8374647.

Hsu, J. P.; Nacu, A. Behavior of soybean oil-in-water emulsion stabilized by nonionic surfactant. *J. Colloid. Interface Sci*. **2003**, *259* (2), 374-81.

Hu, B.; Ting, Y.; Zeng, X.; Huang, Q. Bioactive peptides/chitosan nanoparticles enhance cellular antioxidant activity of (-)-epigallocatechin-3-gallate. *J. Agric. Food Chem.* **2013**, *61* (4), 875-81.

Huth, U. S.; Schubert, R.; Peschka-Süss, R. Investigating the uptake and intracellular fate of pH-sensitive liposomes by flow cytometry and spectral bio-imaging. *J. Control. Release*. **2006**, *110* (3), 490-504.

Iloki-Assanga, S. B.; Lewis-Luján, L. M.; Fernández-Angulo, D.; Gil-Salido, A. A.; Lara-Espinoza, C. L.; Rubio-Pino, J. L. Retino-protective effect of Bucida buceras against oxidative stress induced by H2O2 in human retinal pigment epithelial cells line. *BMC Complement Altern. Med.* **2015**, *15*, 254.

Kamogashira, T.; Hayashi, K.; Fujimoto, C.; Iwasaki, S.; Yamasoba, T. Functionally and morphologically damaged mitochondria observed in auditory cells under senescence-inducing stress. *NPJ Aging Mech. Dis.* **2017**, *3*, 2.

Kim, G. H.; Kim, J. E.; Rhie, S. J.; Yoon, S. The Role of Oxidative Stress in Neurodegenerative Diseases. *Exp. Neurobiol.* **2015**, *24* (4), 325-340.

Lambert, J. D., Yang, C. S. Cancer chemopreventive activity and bioavailability of tea and tea polyphenols, *Mutat. Res.* **2003**, *523-524*, 727–47.

Laudadio, E.; Minnelli, C.; Amici, A.; Massaccesi, L.; Mobbili, G.; Galeazzi, R. Liposomal Formulations for an Efficient Encapsulation of Epigallocatechin-3-gallate: An in-Silico/Experimental Approach. *Molecules*. **2018**, *23* (2), 441.

Laudadio, E.; Mobbili, G.; Minnelli, C.; Massaccesi, L.; Galeazzi, R. Salts Influence Cathechins and Flavonoids Encapsulation in Liposomes: A Molecular Dynamics Investigation. *Mol. Inform*. **2017**, *36*, 11.

Li, G. X.; Chen, Y. K.; Hou, Z.; Xiao, H.; Jin, H.; Lu, G.; Lee, M. J.; Liu, B.; Guan, F.; Yang, Z.; Yu, A.; Yang, C. S. Pro-oxidative activities and dose-response relationship of (-)-epigallocatechin-3-gallate in the inhibition of lung cancer cell growth: a comparative study in vivo and in vitro. *Carcinogenesis*. **2010,** *31* (5), 902-910.

Liang, J.; Cao, L.; Zhang, L.; Wan, X. C. Preparation, Characterization, and In vitro Antitumor Activity of Folate Conjugated Chitosan Coated EGCG Nanoparticles. *Food Sci. Biotechnol*. **2014**, *23* (2), 569-575.

Majno, G.; Joris, I. Apoptosis, oncosis, and necrosis. An overview of cell death. *Am. J. Pathol.* **1995**, *146* (1), 3-15.

Mandel, S. A.; Amit, T.; Weinreb, O.; Youdim, M. B. Understanding the broad-spectrum neuroprotective action profile of green tea polyphenols in aging and neurodegenerative diseases. *J. Alzheimers Dis.* **2011**, *25* (2), 187-208.

Marseglia, L.; Manti, S.; D'Angelo, G.; Nicotera, A.; Parisi, E.; Di Rosa G.; Gitto, E.; Arrigo T. Oxidative stress in obesity: a critical component in human diseases. Int. J. Mol. Sci. **2014**, *16* (1), 378-400.

Mignet, N.; Seguin, J.; Chabot, G. G. Bioavailability of polyphenol liposomes: a challenge ahead. *Pharmaceutics*. **2013**, *5* (3), 457-71.

Milkovic, L.; Siems, W.; Siems, R.; Zarkovic, N. Oxidative stress and antioxidants in carcinogenesis and integrative therapy of cancer. *Curr. Pharm. Des.* **2014**, *20*, 6529-6542.

Minami, H.; Inoue, T. Aggregation of dipalmitoylphosphatidylcholine vesicles induced by some metal ions with high activity for hydrolysis. *Langmuir*. **1999**, *15* (20), 6643–6651.

Minnelli, C.; Cianfruglia, L.; Laudadio, E.; Galeazzi, R.; Pisani, M.; Crucianelli, E.; Bizzaro, D.; Armeni, T.; Mobbili, G. Selective induction of apoptosis in MCF7 cancer-cell by targeted liposomes functionalised with mannose-6-phosphate. *Journal of Drug Targeting*, **2018**, 26(3):1-31.

Mobbili, G.; Crucianelli, E.; Barbon, A.; Marcaccio, M.; Pisani, M.; Dalzini, A.; Ussano, E.; Bortolus, M.; Stipa, P.; Astolfi, P., Liponitroxides: EPR study and their efficacy as antioxidants in lipid membranes, *RSC Adv.*, **2015**, *5*, 98955-66.

Morel, I.; Lescoat, G.; Cogrel, P.; Sergent, O.; Pasdeloup, N.; Brissot, P.; Cillard, P.; Cillard, J. Antioxidant and iron-chelating activities of the flavonoids catechin, quercetin and diosmetin on iron-loaded rat hepatocyte cultures. *Biochem. Pharmacol*. **1993**, *45* (1), 13–19.

Mosmann, T. Rapid colorimetric assay for cellular growth and survival: application to proliferation and cytotoxicity assays. *J. Immunol. Methods.* **1983**, *65*, 55–63.

Müller, R. H.; Maassen, S.; Weyhers, H.; Mehnert, W. Phagocytic uptake and cytotoxicity of solid lipid nanoparticles (SLN) sterically stabilized with poloxamine 908 and poloxamer 407. *J. Drug Target.* **1996**, *4* (3), 161-170.

Nakayama, T.; Hashimoto, T.; Kajiya, K.; Kumazawa, S. Affinity of polyphenols for lipid bilayers. *Biofactors*. **2000**, *13* (1-4), 147-151.

Nanjo, F.; Mori, M.; Goto, K.; Hara, Y. Radical scavenging activity of tea catechins and their related compounds. *Biosci. Biotechnol. Biochem.* **1999**, *63* (9), 1621-1623.

Pabst, G.; Rappolt, M.; Amenitsch, H.; Laggner, P. Structural information from multilamellar liposomes at full hydration: full q-range fitting with high quality x-ray data. *Phys. Rev. E Stat. Phys. Plasmas Fluids Relat. Interdiscip. Topics.* **2000**, *62* (3 Pt B), 4000-4009.

Papahadjopoulos, D.; Jacobson, K.; Nir, S.; Isac, T. Phase transitions in phospholipid vesicles. Fluorescence polarization and permeability measurements concerning the effect of temperature and cholesterol. *Biochim. Biophys. Acta.* **1973**, *311* (3), 330-48.

Price, W. E.; Spitzer, J. C. The kinetics of extraction of individual flavanols and caffeine from a Japanese green tea (Sen Cha Uji Tsuyu) as a function of temperature, *Food. Chem*. **1994**, *50*, 19–23.

Salah, N.; Miller, N. J.; Paganga, G.; Tijburg, L.; Bolwell, G. P.; Rice-Evans, C. Polyphenolic flavanols as scavengers of aqueous phase radicals and as chain-breaking antioxidants. *Arch Biochem. Biophys.* **1995**, *322*, 339–346.

Severino, J. F.; Goodman, B. A.; Kay, C. W.; Stolze, K.; Tunega, D.; Reichenauer, T. G.; Pirker, K. F. Free radicals generated during oxidation of green tea polyphenols: electron paramagnetic resonance spectroscopy combined with density functional theory calculations. *Free Radic. Biol. Med*. **2009**, 46 (8), 1076-1088.

Szoka, F. Jr.; Papahadjopoulos, D. Procedure for preparation of liposomes with large internal aqueous space and high capture by reverse-phase evaporation. *Proc. Natl. Acad. Sci. U. S. A.* **1978**, *75*, (9), 4194-4198.

Tak, P. P.; Zvaifler, N. J.; Green, D. R.; Firestein, G. S. Rheumatoid arthritis and p53: how oxidative stress might alter the course of inflammatory diseases. *Immunol. Today.* **2000**, *21* (2), 78-82.

Torchilin,V.P. Recent advances with liposomes as pharmaceutical carriers. *Nat. Rev. Drug Discov.* **2005**, 4, 145–160.

Wu, G; Khant, H.A; Chiu, W.; Lee K.Y.C. Effects of bilayer phases on phospholipid-poloxamer interactions. *Soft matter*. **2009**, *5*, 1496-1503.

Zareba, M.; Raciti, M. W.; Henry, M. M.; Sarna, T.; Burke, J. M. Oxidative stress in ARPE-19 cultures: do melanosomes confer cytoprotection? *Free Radic. Biol. Med.* **2006**, *40* (1), 87-100.

Zhang, B.; Safa, R.; Rusciano, D.; Osborne, N. N. Epigallocatechin gallate, an active ingredient from green tea, attenuates damaging influences to the retina caused by ischemia/reperfusion. *Brain Res*. **2007**, *1159*, 40–53.